Proceedings of
2003 STLE/ASME International Joint Tribology Conference
Ponte Vedra Beach, Florida USA, October 26–29, 2003

2003TRIB-269

A CYLINDRICAL CONTACT MODEL FOR TWO DIMENSIONAL MULTIASPERITY PROFILES

John J. Jagodnik and Sinan Müftü
Northeastern University
Department of Mechanical Engineering
Boston, MA 02115

ABSTRACT

In practice, multi-asperity contact problems are often solved as two dimensional (2D) plane problems rather than true three dimensional (3D) problems. This is accomplished by assuming that each peak on a 2D scanned profile is the pinnacle of a half sphere. Hertz contact equations are then used to solve for the radius of contact and pressure profile. In reality, the local maximum in the plane may not be the maximum in the unmeasured depth direction, creating inherent errors in the contact model. This error is shown to be significant in contact problems when estimating the area of contact and total contact force over a single asperity. The pressure corrected Sternberg-Turteltaub model is introduced, in which a cylinder is used to model a sphere in a plane. This model is shown to improve the contact area and total force estimates for a range contact parameters.

INTRODUCTION

Typically, multi-asperity contact problems are solved by assuming that each asperity is a perfect sphere. Hertz's equations for contacting spheres gives good estimates of the contact pressure profile, if the radius of the sphere is known [1]. However, the topography of the surface is often measured by using a stylus type profiler, which scans a single plane. In reality, the local maximum in the scanned plane may not be the maximum in the unmeasured depth direction. Using this radius in the spherical Hertz contact model creates inherent errors. In this paper the significance and reasoning behind these errors are introduced and corrections, including a modified form of the cylindrical contact model, are proposed to reduce the error in plane approximations.

Plane Approximations

Multi-asperity contact problems can be solved in two or three dimensions. A surface profiler can be used to determine the surface height in both the x and y directions (Fig 1). Then, the overall equilibrium of the two contacting surfaces could be found by direct modeling of each asperity as Hertz contacts [1], or by statistical techniques [2]. For these problems, each asperity is treated as a sphere and Hertz contact equations are applied. Typically, 3D solutions require significant computational time. It is also difficult to analyze complex problems involving sliding, composite layers, etc. in 3D [4].

Two dimensional (2D) "plane approximations" provide an alternative, where a surface profiler could be used to obtain the surface heights along the x direction, on a single x-z plane, as shown in Fig 1. Similar profiles can be obtained for a general surface using a random profile generator [3]. Typically each peak on the profile is treated as the pinnacle of a sphere and Hertz contact equations are applied. In this paper, we will investigate the error from ignoring the y direction effects when a 2D profile is analyzed, rather than a full 3D surface.

THEORY

Single Asperity Analysis

Here a single asperity rather than an entire surface or profile is analyzed. The asperity is treated as a perfect half sphere, whose center lies in a plane-1 as shown in Fig 2a. The sphere is subjected to interference from a flat rigid punch. It will be assumed that the surface profiler scanned the asperity along plane-2, which is parallel to plane-1, but offset by a distance y^*.

Focusing on a front view of the asperity in Fig 2b, it is

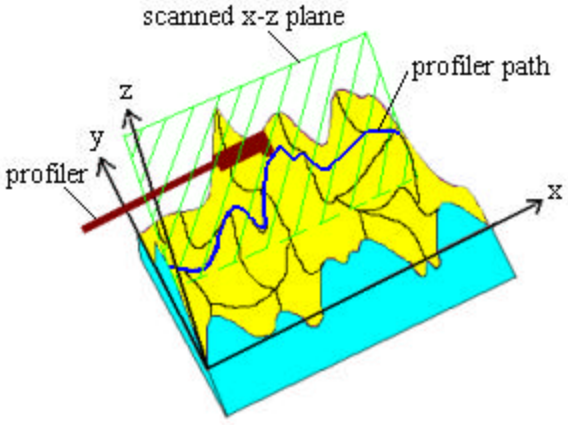

Figure 1 3D plane profile, and the 2D profile in the x-z scan plane

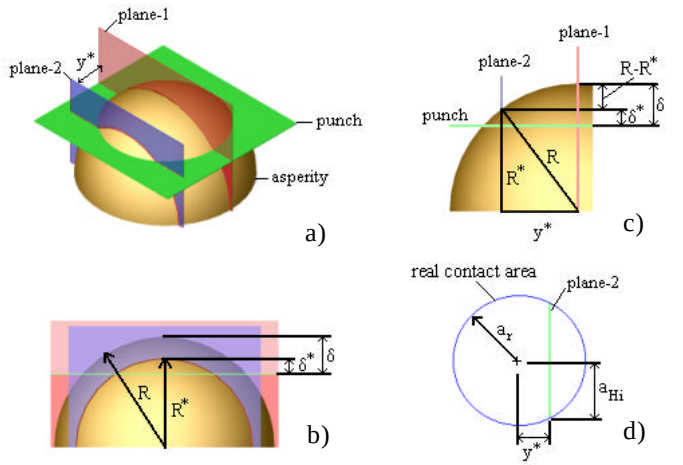

Figure 2: a) Three dimensional model of an asperity; The front b) and side c) views; and d) Details of the real contact area.

noted that if the scan plane is identical to plane-1, the true radius of the sphere (R) and the true maximum interference (δ) will be found. If y^* is not zero, a different value for the radius (R^*) and maximum interference (δ) will be observed. Clearly assuming that the observed half circle on the scanned profile is the pinnacle of a sphere will lead to some amount of error depending on the value of y^*.

Focusing on Fig 2c, the relationships between the true and observed radii and maximum interferences are found as follows,

$$\delta^* = \delta - \left(R - R^*\right) \text{ (a)}, \qquad R^* = \sqrt{R^2 - y^{*2}} \text{ (b)} \qquad (1)$$

Analysis Over The Entire Asperity

In order to gain valuable information about the error associated with using the parameters obtained from a line scan, the entire asperity will be analyzed, rather than simply analyzing a single y^* value. In order to do this, n (=200) equally spaced y^* values are selected. These y^* values cover the entire range, where the punch interferes with the undeformed sphere. For each y^* value the contact problem is solved on plane-2 using three methods.

First, the full 3D model is solved using spherical Hertz contact equations with the true radius and true maximum interference from plane-1. The relevant information for plane-2 is then extracted from the 3D solution. This approach is called the Hertz (H) model.

The second method for solving the plane problem is to simply apply the spherical Hertz contact equations to the perceived radius R^* and interference δ^* value, obtained from the profile. This approach, which is based on incomplete information on surface topography is called the incomplete Hertz (Hi) model.

The third method involves using a modified form of the *cylindrical contact* model based on Sternberg and Turteltaub's (ST) work [5]. This model provides a relation between the punch penetration δ and the contact radius a, and cylinder radius R. The modified ST model is introduced later in the paper. The values of R^* and δ^* obtained from the profile are used in the ST equations. This modified cylindrical contact model is called the ST-model, here.

Equations for the Three Models

The focus of the analysis is to determine the cumulative effect of randomly chosen plane-2 (y^*) locations on the spanned contact area (A_j) and total force (F_j), using the three methods. A different subscript j used on the variables, to indicate the method. The subscript $_H$ is added for the real 3D Hertz solution. The subscripts $_{Hi}$ and $_{ST}$ are used for the incomplete Hertz model and for the cylindrical contact with Sternberg-Turtlebaum's modifications, respectively. The radius and punch penetration values in the last two models are obtained in plane-2.

Equations for the Real 3D Hertz Solution

The relation between the true contact radius a_r and the perceived contact radius a^*_{Hi} can be found from Fig. 2d as,

$$a^*_{Hi} = \sqrt{a_r^2 - y^{*2}} \,. \qquad (2)$$

Substituting the well-known Hertz [1] relationship between contact radius and maximum interference ($a_r^2 = R\delta$), the real contact radius on any plane can be found to be,

$$a^*_{Hi} = \sqrt{R\delta - y^{*2}} \,. \qquad (3)$$

Using the pressure distribution from Hertz contact, the equation for the pressure in the contact length (x) of the scan plane is,

$$p_H(x) = \frac{2E\delta}{\pi\left(1-\nu^2\right)a_r}\sqrt{1-\frac{x^2+y^{*2}}{a_r^2}} \,. \qquad (4)$$

The force per unit width on the scan plane $\left(F'_H\right)$ is found as,

$$F'_{Hr} = \frac{E\delta}{1-\nu^2}\left(1-\frac{y^{*2}}{a_r^2}\right), \qquad (5)$$

by integrating p_H over the real contact length for the scan plane-2.

The spanned contact area (A_H) is found by numerically integrating the contact length $2a^*_r$ through the y direction with,

$$A_H = 2\Delta y^* \sum_{i=1}^{n}\sqrt{R\delta - y_i^{*2}} \,. \qquad (6)$$

where n is the number of line scan locations.

Similarly, the total force applied to the asperity is found by numerically integrating F'_H through the y^* direction with,

$$F_r = \frac{E\delta\Delta y^*}{\left(1-\nu^2\right)}\sum_{i=1}^{n}\left(1-\frac{y_i^{*2}}{a_r^2}\right). \qquad (7)$$

In these summations, Δy^* is the spacing between scan planes in the y direction. It should also be noted that the Hertz equations can be applied directly to find the true contact area and force supported by the asperity without numerical integration. These equations can be used to verify that a small enough Δy^* value has been selected.

Equations for the Incomplete Hertz Model

For the Hertz sphere solution, the radius of contact on any scan plane is given as,

$$a^*_{Hi} = \sqrt{R^*\delta^*}\,. \tag{8}$$

where R^* and δ^* are given in Eqns (1a) and (1b).

The contact area is found by integrating in the y^* direction in the same manner that was followed for the 3D solution, giving,

$$A_{Hi} = 2\Delta y^* \sum_{i=1}^{n} \left(R^*\delta^*\right)^{1/2}. \tag{9}$$

The pressure at a given x value in the contact length on a scan plane is,

$$p_{Hi}(x) = \frac{2E\delta^*}{\pi\left(1-\nu^2\right)a^*_{Hi}} \sqrt{1-\left(\frac{x}{a^*_{Hi}}\right)^2}\,. \tag{10}$$

The force per unit width on the scan plane can be found by integrating p_{Hi} over the contact length for the scan plane. Performing this integration leads the force per unit width, given as,

$$F'_{Hi} = \frac{E\delta^*}{1-\nu^2}. \tag{11}$$

Numerical integration through the entire asperity in the y direction leads to the total force on the asperity, given as,

$$F_{Hi} = \frac{E\Delta y^*}{1-\nu^2} \sum_{i=1}^{n} \delta^*_i\,. \tag{12}$$

Equations for the Cylindrical Contact with Sternberg-Turteltaub Modifications

Sternberg and Turteltaub analyzed an infinitely long cylinder with a finite radius R compressed a distance 2δ between two flat rigid punches [5]. From this analysis the following equations were obtained under the assumption that radius of the cylinder R is much greater than the half-contact length a,

$$\frac{\delta}{R} = \frac{\gamma^2}{2}\left(\ln\left[\frac{4}{\gamma}\right] - \frac{1}{2}\right) + \frac{9\gamma^4}{64}$$

$$\frac{a}{R} = \gamma - \frac{\varphi\gamma^2}{4} \tag{13a,b,c}$$

$$\upsilon p^s_o = \gamma + \frac{3\gamma^3}{16}$$

where p^s_o is the maximum contact pressure, $g = \left(2uP/pR\right)^{1/2}$, $\upsilon = 2\left(1-\nu^2\right)/E$, and $\varphi = \left(1-2\nu\right)/2\left(1-\nu\right)$.

Using symmetry about the mid-plane between the two punches allows the problem to be treated as a half cylinder. In this work Eqns (13a) and (13b) are solved numerically by using ν = 0.3, and a curve fit relationship between a, R, and δ is obtained,

$$a = C_s R^{1-m}\hat{\delta}^m \tag{14}$$

with C_s = 0.962 and m = 0.557. Note that this equation is valid in the range $1.15\times10^{-6} \le \delta/R \le 2.25\times10^{-3}$. Substituting eqns (1a) and (1b) yield the half-contact length,

$$a^*_{ST} = 0.962R^{*0.443}\,\delta^{*0.557}. \tag{15}$$

The contact area is obtained, by numerically integrating through the y direction,

$$A_{ST} = 1.924\Delta y^* \sum_{i=1}^{n} R^{*0.413}\delta^{*0.557}\,. \tag{16}$$

The pressure at any point in the contact length on a scan plane is represented by,

$$p_{ST}(x) = \frac{E}{1-\nu^2}\left(\eta + \frac{3}{4}\eta^3\right)\left[1-\left(\frac{x}{a^*_{ST}}\right)^2\right]^{1/2} \tag{17}$$

where,

$$\eta = \frac{1}{\varphi}\left[1-\left(1-\varphi\frac{a^*_{ST}}{R^*}\right)^{1/2}\right]. \tag{18}$$

The force per unit width on the scan plane for the ST cylinder is found in the same manner as the Hertz analysis,

$$F'_{ST} = 0.481\pi\frac{E}{1-\nu^2}R^{*0.443}\delta^{*0.557}\left(\eta + \frac{3}{4}\eta^3\right). \tag{19}$$

The total force on the asperity is found as,

$$F_{ST} = 0.481\pi\frac{E\Delta y^*}{1-\nu^2}\sum_{i=1}^{n} R^{*0.443}\delta^{*0.557}\left(\eta_i + \frac{3}{4}\eta_i^3\right). \tag{20}$$

Non-dimensional Equations

All of the variables involving a length are scaled with a_r,

$$\bar{a}^*_j = \frac{a^*_j}{a_r},\ \bar{R}^* = \frac{R^*}{a_r}, \bar{R} = \frac{R}{a_r}, \bar{\delta}^* = \frac{\delta^*}{a_r},\ \bar{\delta} = \frac{\delta}{a_r},$$

$$\bar{y}^* = \frac{y^*}{a_r}, \bar{F}'_j = \frac{F'_j}{p_o a_r}, \bar{F}_j = \frac{F_j}{p_o a_r^2},\ \bar{p}_j = \frac{p_j}{p_o} \tag{21}$$

where the subscript j takes the values $_H$, $_{Hi}$ and $_{ST}$ as appropriate, and the maximum pressure is defined as,

$$p_o = \frac{2Ed}{p\,a_r\left(1-n^2\right)}. \tag{22}$$

This non-dimensionalization results in only three independent parameters that control the problem, ν, $\bar{R}$ and $\bar{y}^*$.

RESULTS

Contact Pressure

The contact pressure distribution for the three models are plotted for three different $\bar{y}^*$ values and $\bar{R}$ =110 in Fig 3. This figure shows that the Hi- and the ST-models approach the Hertz pressure distribution as $\bar{y}^* \to 0$ and $\bar{y}^* \to 1$, respectively. This indicates that, as the line-scan moves further away from the pinnacle of the asperity, the match between the ST and Hertz models gradually improves.

Contact Radius

Contact radius $\bar{a}$ is plotted for different $\bar{y}^*$ locations and $\bar{R}$ values in Figure 4a. The contact radius $\bar{a}_H$ for the Hertz solution falls on a unit circle as expected. However, the contact radius of the Hi-model ($\bar{a}_{Hi}$) overestimates and the contact radius of the ST model ($\bar{a}_{ST}$) underestimates the Hertz solution. It is interesting to note that the effect of asperity radius $\bar{R}$ on the Hi-model is so small that it can not be detected in Fig. 4a. On the other hand the ST-model further underestimates the contact radius with increasing $\bar{R}$.

Contact Area Span

The probability of scanning a given asperity at a $\bar{y}^*$ location is the same for all $\bar{y}^*$ values. Therefore, if we integrate the area under the $\bar{a}$ curve, given in Fig 4a, we get an estimate of the contact area span A_j that the three models are capable of estimating.

A_j is obtained numerically from eqns (6), (9) and (16). Figure 4b displays the A_j values for all three methods. Note that the spanned area for the Hertz model is the constant π, and is equal to the real contact area of the Hertz contact model with the non-dimensional contact radius of 1. The spanned area for the Hi-model is nearly constant with 4.53. This value is 44% greater than π. Finally, the spanned area of the ST-model is variable as shown in Fig 4b. The error between spanned area estimates of the Hertz model (π) and the ST-model varies between 3% and 30%, where the error becomes smaller at smaller values of $\bar{R}$.

When using plane approximations, the Hi- and ST-models wrongly assume the sphere or the cylinder is centered on the scan plane and thus the first point to touch the flat punch is the peak as seen in the scan plane. This reasoning explains the overshoot area for the Hi- and ST-models. The remaining error in the ST-model is simply attributed to modeling a portion of a sphere with a cylinder.

While it may not be apparent as to why the ST cylindrical model is being considered for modeling spheres in a plane, it is interesting to note that the this model provides a better approximation to the true contact area in the range of asperity radii ($15 \le \bar{R} \le 250$) considered in Fig. 4b. This is a result of the underestimation of the contact radius near the center of the sphere, which to some extent corrects the overestimation in the overshoot area. This correction is lacking in the Hi-model where the contact radius is overestimated at all points except the center where the solution is precise.

Force per Width

The force per width $\bar{F}_j'$ expressions, for the three models, are given in equations (5), (11) and (19). These expressions are plotted in Fig 5a as a function of scan location $\bar{y}^*$, for three different values of $\bar{R}$. This figure shows that the force per width is overestimated by the Hi-model as compared to the Hertz model; and, it is underestimated by the ST-model for a large section of the $\bar{y}^*$ range. The Hi-model is insensitive to changes in $\bar{R}$, whereas the estimate of the ST-model becomes worse as $\bar{R}$ increases.

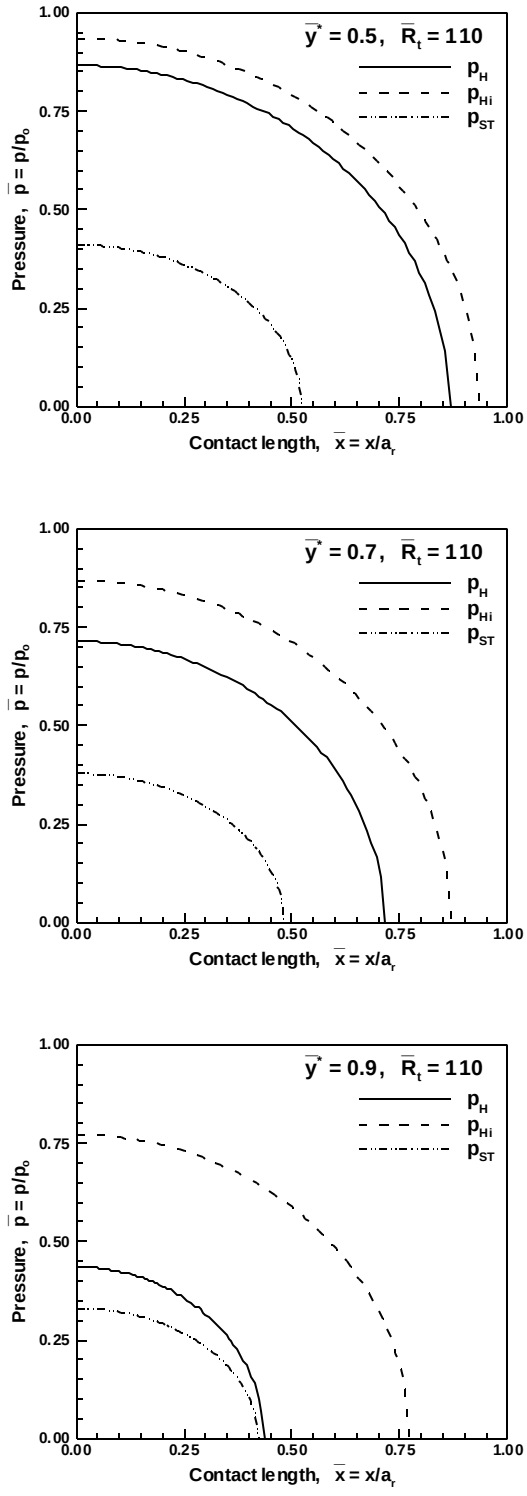

Figure 3 Contact pressure distribution for $\bar{y}^*$ =0.5, 0.7, 0.9 and $\bar{R}$ =110.

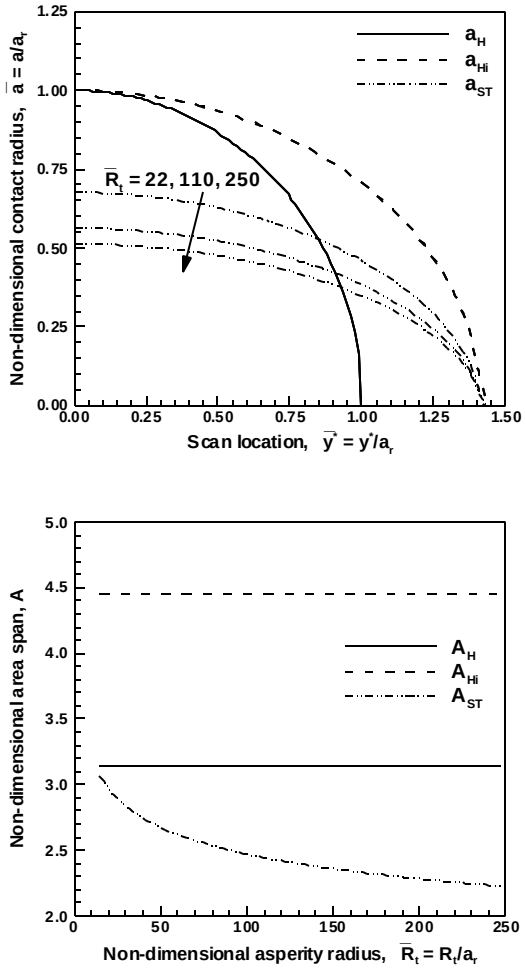

Figure 4 a) Non-dimensional contact radius for different $\bar{R}$ values. b) Contact area span variation with $\bar{R}$ for the three models.

Total Force

As was the case for the spanned contact area, we can view the effects of asperity radius $\bar{R}$ on the total spanned force $\bar{F}_j$. Eqns (6), (13) and (20), which give the $\bar{F}_j$ expressions for the three models, are plotted in Fig 5b. This figure shows that $\bar{F}_H$ = 1.05 for the Hertz model, and that it is independent of $\bar{R}$. The total force for the Hi-model is nearly constant with the value $\bar{F}_{Hi}$ = 1.49. However, the total force for the ST-model varies with $\bar{R}$ as shown in Fig 5b. The error between the ST-model and the Hertz solution varies between 52 and 71%.

The error between the total force estimates can be reduced by introducing correction factors for the pressure estimates given by eqns (10) and (17) for the Hi- and ST-models, respectively. Fig 5b suggests that a constant correction factor of C_{Hi} = 0.7 should be used for the Hi-model. On the other hand the correction factor C_{ST} for the ST-model depends on the value of $\bar{R}$. For example, we found that for $\bar{R}$ =110 the correction factor should be C_{ST} = 2.8. The value of $\bar{R}$ =110 represents, for

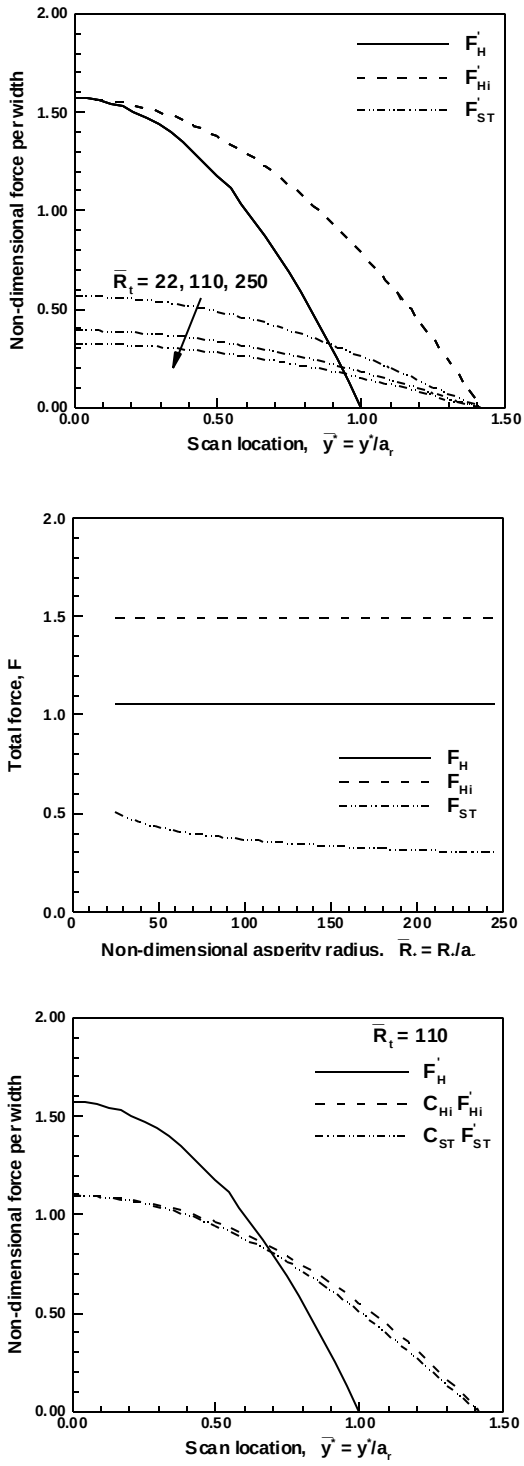

Figure 5 a) Dimensionless force per width as a function of scan location $\bar{y}^*$. b) Total spanned asperity force as a function of asperity radius. c) Estimates of the Hi and ST models with correction factors C_{Hi} and C_{ST}.

example, R = 121 μm and δ = 10 nm, which are parameters typical of magnetic tape applications [4].

Fig 5c shows the effect of using the correction factors indicated above on the estimates of force per width of the asperity. Both the Hi- and ST-models follow very similar

trends, and the areas under the two modified curves nearly equals that under the H-model.

It is also important to note that the pressure correction factors do not effect the contact area analysis stated above. Therefore, the errors in contact area estimation remain as they are given in Fig 4b. As the area estimate errors are smaller for the ST-model, as compared to the Hi-model use of the ST-model may be an attractive choice.

DISCUSSION

Qualitative Analysis of Multi-asperity Contact

In the previous sections contact over a single asperity was analyzed. While this analysis provides insight into the reasoning behind the use of the pressure corrected ST model, the real purpose for using either model is to analyze a single plane from a multi-asperity surface.

In the previous section a single asperity was broken into 200 thin strips. Each strip was analyzed and then combined to find the resulting area of contact and total force approximations. The behavior of a plane from a multi-asperity contact problem closely parallels the single asperity analysis.

Let us consider a scan plane, which intersects n contacting asperities, and assume the y coordinates for the centers of each asperity are random and uncorrelated. If this is the case there is an equal probability for any one of the 200 thin strips of a given asperity falls within the scan plane. This means that if n is large, we expect to see n/200 strip 1s, n/200 strip 2s, etc. This is close to analyzing n/200 single asperities, with the only difference being the variation of $\overline{\delta}/\overline{R}$ from asperity to asperity due to the random nature of the surface. Neglecting the effects of the variation in $\overline{\delta}/\overline{R}$, the conclusions reached for a single asperity can be directly applied to the multi-asperity contact case. While this qualitative analysis appears reasonable, a more detailed quantitative analysis of multi-asperity plane approximations will be the subject of a future paper.

SUMMARY AND CONCLUSION

While the accuracy of the Hertz contact equations are uncontested in a 3D analysis, often the equations are used with information based on 2D plane scans. In these analyses, the local peaks are assumed to be the pinnacles of a sphere, when in fact they may not be the pinnacle had the depth direction been considered. The errors for this assumption have been analyzed for a single asperity and shown to be substantial when estimating the contact area and total force over the asperity. Correction factors for the contact pressure are discussed. In particular, a modified (ST) cylindrical contact model is introduced. This model is shown to be better in predicting contact area. A more robust model for determining the pressure correction factor and a more vigorous multi-asperity contact analysis will be the subject of future papers.

REFERENCES

1. Johnson, K.L. (1985) *Contact Mechanics*, Cambridge University Press.
2. Greenwood, J.A. and Williamson, J.B.P. (1966) "Contact of Nominally Flat Surfaces," *Proceedings, Royal Society*, **A295**, 300.
3. Patir, N. (1978) "Numerical Procedure for Random Generation of Rough Surfaces," *Wear*, v 47, n 2, 263.
4. Bhushan, B. (1996) *Tribology and Mechanics of Magnetic Storage Devices*, Springer- Verlag New York Inc., New York (Ch. 2 and 3).
5. Gladwell, G.M.L. (1980) *Contact Problems in the Classical Theory of Elasticity*, Sijthoff & Noordhoff Int. Publishers, The Netherlands (Ch. 8).